A framework for multi-fidelity multi-disciplinary kriging-based surrogate model optimization of novel aircraft configurations

Martin Sohst
Jose Vale, PhD
Curran Crawford, PhD
University of Victoria
CANADA

msohst@uvic.ca

Graham Potter
Sid Banerjee
Bombardier Aerospace
CANADA

Keywords: Multi-disciplinary design optimization, Aeroelasticity, Multi-fidelity, Novel aircraft, Surrogate model

ABSTRACT

A novel Strut-Braced Wing (SBW) configuration is compared to a cantilevered High Aspect Ratio Wing (HARW) based on the Predator drone. Both configurations are optimized for maximum load factor bearing capability subject to a maximum mass, maximum structural stress and minimum aerodynamic efficiency (L/D) constraints. The optimization resorts to the generation of kriging based surrogate models for the different parameters involved. The sampling of the results is generated using a Fluid-Structure Interaction (FSI) procedure that couples an Equivalent Beam Model with Low Fidelity (Panel Method) or High Fidelity (RANS) aerodynamics. The generation of HF samples is attempted to be minimized using engineering judgment. Nevertheless, the dimensionality of the SBW optimization problem seems to require additional samples to improve the quality of the surrogate models. Results show that the proposed configuration does not seem suitable to increase the load bearing capability without penalizing structural mass and/or aerodynamic efficiency. The main reason for such difficulties is that although an increase in the wing Aspect Ratio (AR) allows to neutralize the drag penalty due to the presence of the strut, the deformation of the structure induces extra drag penalty.

1.0 INTRODUCTION

Aerodynamic efficiency and structural weight reduction are two aircraft design requirements not easy to comply with simultaneously. Nevertheless, the novel aircraft configurations proposed in the recent past are following the direction of more deformable structures as an outcome of increasing the aircraft's aspect ratio (AR) while avoiding significant structural mass penalties. Examples of such configurations include High Aspect Ratio Wings (HARW), Joined Wings (JW), Struct Braced Wings (SBW) among others (Abbas et al., 2013; Carrier et al., 2012; Cavallaro and Demasi, 2016; Wolkovitch, 1986).

As a result of these higher levels of deformation, a sufficiently accurate prediction of the aircraft's deformed shape is required to ensure that the expected aerodynamic benefits are not impaired by the actual in-flight shape. Static Fluid-Structure Interaction (FSI) analysis procedures (Dowell et al., 2003) can be used for this purpose, where different aerodynamic and structural analysis modules are coupled together to obtain a converged load-deformation combination as the solution for a specific flight condition.

Depending on the flight condition the convergence of the FSI procedure may be faster or slower. Higher load and/or deformation tend to require a higher number of iterations to achieve convergence. This may also mean

high computational time or resources for an analysis, particularly if high fidelity models are required to assess the benefits of a configuration. This is in general the case when aerodynamic efficiency (therefore drag) is required to be quantified with an acceptable level of accuracy and a typical aerodynamic tool is used with a RANS (Reynolds Averaged Navier-Stokes) solver and an available turbulence model.

In the event of using an aero-structural optimization procedure to obtain, assess and compare different configurations a direct approach based on High Fidelity (HF) FSI becomes too expensive, independently of the optimization algorithm choice or strategy (gradient based, genetic algorithm etc.) chosen (Wang and Shan, 2007)

An alternative approach to tackle this problem can be using surrogate models for the computation of the approximate values of the required quantities to calculate the objective function and constraints values. Some surrogate model formulations are available in the literature, for instance polynomial regression, radial-basis functions, kriging, neural networks, etc (Forrester et al., 2008; Wang and Shan, 2007). Based on a set of results for a sample of design variables, surrogate models can be built and used for a small computational cost in an optimization procedure. The drawbacks arise from the accuracy of the models being dependent on the size of the sample pool and on the dispersion of the sample.

Although once calculated the models are cheap to use, obtaining an accurate model with the least amount of samples possible is not free of challenges. One usual approach is to improve the surrogate models by adding samples to the model. Automated criteria for determining which should be the next sample point added to the sample pool, e.g. mean squared error (MSE), Expected Improvement (EI) or a combination of those (Biles et al., 2007; Kleijnen et al., 2012), can be implemented to explore the design space, while using the optimum result from an optimization based on these models as a new sample point serves simultaneously to check the accuracy of the model predictions as well as to increase the number of sample points. A balance between exploration and exploitation of the design space is sought in order to improve the quality of the models in the regions of interest (Forrester et al., 2008).

Another strategy to reduce the number of HF evaluations consists of using Lower Fidelity (LF) models to explore the design space and restrict the HF evaluations to the most promising designs and confirmation of optimal results. This is the multi-fidelity approach to the optimization, where an error surrogate model is built to predict the differences between HF and LF models (Zhang et al., 2018).

In this paper, a configuration based on the Predator drone with an aspect ratio of 22 is compared to an SBW configuration. Both configurations are optimized for maximum load factor capability with minimum range and maximum stress constraints, using Kriging-based multi-fidelity and multi-disciplinary optimization considering FSI results from LF and HF aerodynamic solvers.

In section 2.0, the Multidisciplinary analysis framework and models used for this comparison is described. Section 3.0 details the optimization problems for the two different configurations and Section 4.0 discusses the surrogate models generation and sample management. Section 5.0 shows the results obtained and compares the two optimized configurations. Finally, Section 5.0 summarizes the findings and the final conclusion of this work. Sections 6.0 and 7.0 present the references and acknowledgments, respectively.

2.0 FRAMEWORK DESCRIPTION

2.1 Multi-Disciplinary Analysis (MDA)

An in-house tool is used to perform static FSI analysis on the aircraft configurations. This tool used a structural Equivalent Beam Model (EBM) coupled with either a LF or a HF aerodynamic model.

Lifting surfaces are assumed to have a wingbox type structure and the fuselage is assumed to behave like a rigid beam. The model extracts the sectional properties of the wingbox sections and translates those into a

Timoshenko beam model. With the EBM model, the wingbox mass can be obtained, as well as the Von-Mises stress distribution on the beam elements representing the aircraft structure. The model is then used for linear analysis once the loading is defined.

The LF aerodynamic model consists of a Panel Method (PM) model that includes fuselage, wing and tail components and calculates the lift and induced drag of the configuration. A friction drag correction is added to the calculations based on flat plate boundary layer models. Although fairly accurate to predict lift in the linear range of angles of attack (AOA), the model is not suitable to accurately predict drag or separation. More detailed descriptions of these models can be found in (Katz and and Plotkin, 2004).

The HF aerodynamics uses a commercial software is used to perform RANS simulations of the aircraft configurations. This software is capable of more accurate drag predictions and accounts for the aerodynamic non-linearities related to the boundary layer (Sigrist, 2015).

Payload and system masses and their inertial components are user inputs and modelled as mass points with inertia and are rigidly connected to the closest structural node. Again, a more detailed description of such modelling can be found in (Oden, 1975).

The static FSI procedure couples aerodynamic and structural models using an iterative procedure where the structural deformation affects the mass distribution and external geometry of the aircraft, which is then meshed and analysed by the aerodynamic solver to get a new load and recalculate deformation. The procedure is considered converged when there is no significant change in the deformation after consecutive iterations. During the procedure, the fuel, payload and systems mass distribution is also affected by the structural deformation.

During the FSI analysis the structure is clamped at the CG location. The aerodynamic loads will not trim the aircraft in general. As a consequence, the effect of the trim in the wing loads and deformation are being neglected in these analyses. The computational effort required to include these effects in the analyses was considered excessive for the purpose of this study. Propulsion effects in the aerodynamics are also neglected in this study. The analysed configurations consist of a pusher propeller engine that due to its position should not have a significant impact on the flow over the wing and tail.

2.1.1 Multi-fidelity FSI calculations

For low subsonic flight, the PM model predicts the lift distribution with a fair degree of accuracy in flows without significant separation. Taking advantage of this fact, one can expedite the HF FSI calculation by using HF aerodynamics only after the LF FSI has converged, since lift is accurately predicted and is the major factor at play in obtaining the structural model deformation. Therefore, the HF FSI consists of one FSI iteration on the converged LF FSI result unless the differences in deformation are deemed significant.

2.2 Surrogate Models Generation

The previous procedure for MDA is used to obtain several parameters of interest for a configuration with a specific set of design variables: structural weight; Lift (L), Drag (D), Deformation and Stress distribution for several Angles of Attack (AOA). These are the parameters required for the optimization of the configurations described below.

2.2.1 Sampling of results

The initial sampling of the design variables is based on the space filling Latin Hypercube sampling (LHS) method. This is the method that ensures a sufficient dispersion of the samples to cover the design space. The number of samples is set to five times the numbers of design variables (8) for the baseline HARW (40) and to four times the number of design variables for the SBW (20), respectively. This way an adequate pool is generated with a reasonable computational cost.

2.2.2 Kriging Surrogate

To overcome the heavy computational costs of an optimization employing a gradient based approach or a genetic algorithm a surrogate model-based optimization approach is chosen. Between the different choices Kriging was selected as it provides predictions based on fewer number of samples compared to other surrogate models if the number of design variables is not excessive (Forrester et al., 2008).

It is a spatial analysis method, considering a global low order regression, paired with local deviations based on covariances between the samples to fit and interpolate the data. The quality of the generated surrogate is contingent on the sample quality. Depending on the size of the pool and number of design variables, different approaches can be used. In Ordinary Kriging, the global model is assumed constant and the samples are interpolated in between. In Universal Kriging the mean value is a higher order polynomial. In the literature it can be found that Ordinary Kriging performs satisfying with frequently providing better results than Universal Kriging. In the present work for every surrogate model it is determined via a cross validation which approach is more suitable.

2.3 Multi-disciplinary Design Optimization Procedure

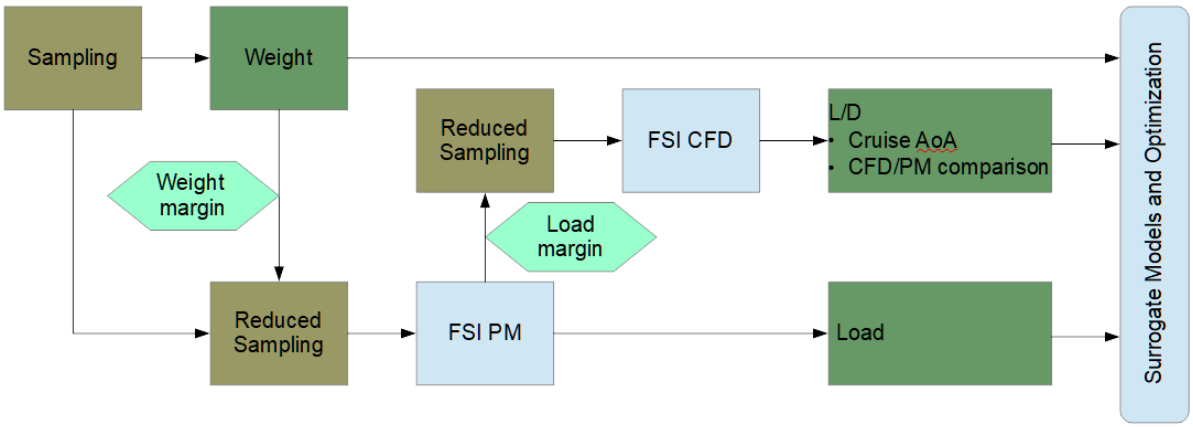

Figure 1: Process of the Multi-Disciplinary Design Optimization (MDO) process

In Figure 1 the process is shown of the chosen MDO procedure. It was started with an initial data base of samples to represent the design space of interest. For those samples the respective weight was determined, and it was decided which of the samples are candidates for the aeroelastic analysis. Following, the FSI was used to compute the maximum load and stress distribution. Promising samples were taken further in the process for a high fidelity CFD analysis to determine the drag and therefore the L/D at cruise flight condition. This led to a database of samples for which the load, weight and aerodynamic properties where gained and which built the base for the surrogate model. Within the optimization process, surrogate models were built for those properties and new sampling points were chosen according to the predictions. This way, design space was explored in a more efficient way in regions of interest, where the number of samples could be reduced for increasing fidelity evaluations.

3.0 MDO OF CONFIGURATIONS DESCRIPTION

Two configurations are being compared in this work. One is based on the Predator drone geometry and performance metrics publicly available and some assumed characteristics as aerofoils geometry and internal structure topology. This configuration is assumed as the baseline to compare the next configuration to.

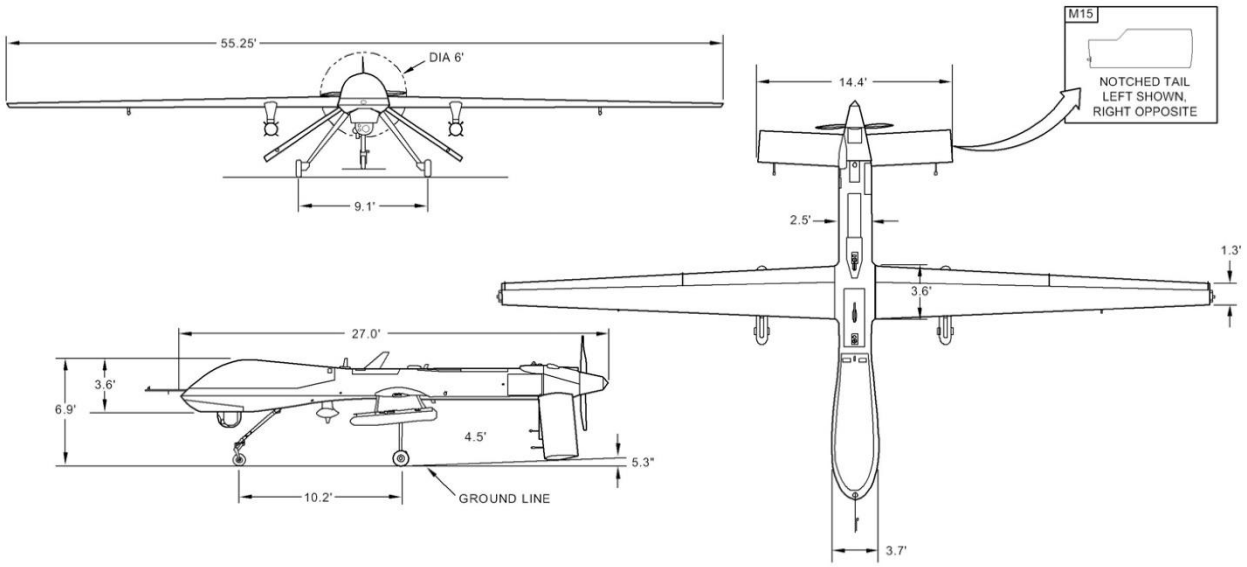

Figure 2: 3 view drawing of the Predator drone used as a baseline for this study [1]

Figure 2 depicts a 3-view drawing of the Predator drone. As one can see, the configuration consists of a cantilevered HARW and an inverted V-tail. The dimensions of the aircraft wing, fuselage and tail were used to generate the baseline model. Some specifications for this aircraft are shown in Table 1.

Table 1: Specifications for the baseline configuration based on publicly available information [1].

Component	Value
Length [m]	8.23
Half-span [m]	8.42
Root chord [m]	1.148
Tip chord [m]	0.396
Taper ratio	0.345
MTOW [Kg]	1020
MFW [Kg]	300
Cruise speed [Km/h]	130-170
Maximum Speed [Km/h]	217
Cruise Altitude [m]	4600

The second configuration is a variation of the baseline that has a strut connecting the main wing to the tail, which has been replaced by an inverted T-tail. Figure 3 shows a view of the proposed configuration.

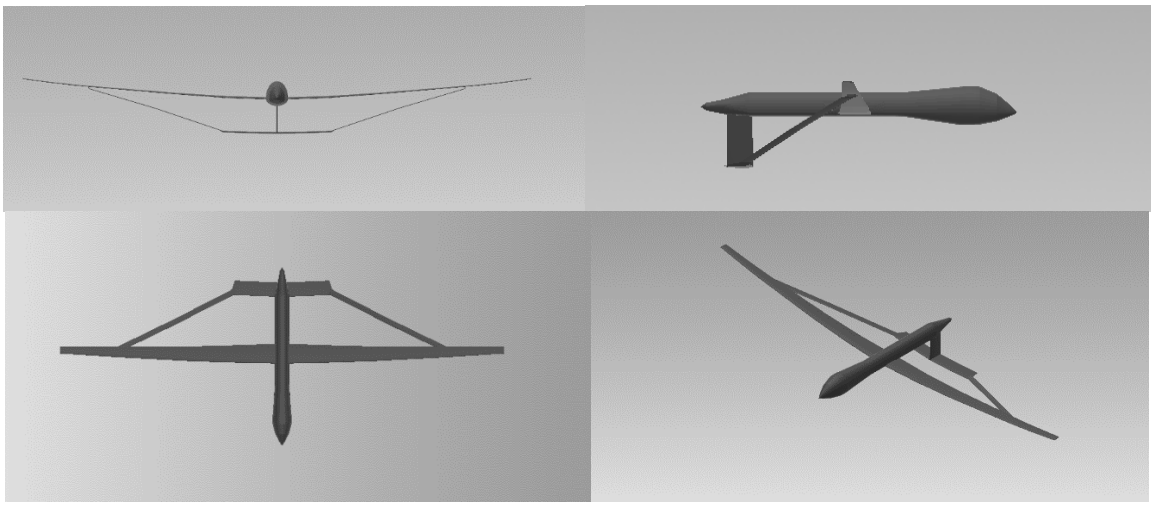

Figure 3: Proposed configuration to increase manoeuvrability

The potential benefits of an SBW configuration are usually based on the increase on aspect ratio and consequent reduction in induced drag that such a configuration supposedly would allow, at the expense of the extra structural member which is the strut. This member would contribute to structural weight and aerodynamic drag, which would be overcome by the benefits of lower main wing structural mass and lower induced drag. The overall outcome would be a higher L/D ratio and better aerodynamic efficiency. These are usually the goals for commercial aircraft in order to save operational costs (fuel).

For a military application for which an existing aircraft already provides sufficient performance (*p.e.* range), it might be of interest to improve other performance metrics, as manoeuvrability. Therefore, in this work we will be comparing the SBW configuration with the baseline configuration in terms of maximum load bearing capability while maintaining or increasing the baseline range (L/D) and maintaining or decreasing the baseline wing's structural weight.

3.1 Baseline Configuration MDO

The Baseline configuration is not completely defined. The available information provides the wing planform and tail dimensions. The remaining information required for a complete outer shape definition is the aerofoils geometry for wing and tail and the twist distribution. In this work, the aerofoil shapes are assumed to be transitioning linearly with span from SD7032 at the root to SD7037 at the tip. The tail aerofoil is assumed as a constant NACA0010 shape. The tail is assumed to have no twist along the span.

On the structural side, the wing and tail structures are assumed to be of a wingbox type, and their chord wise extensions are fixed. The relative chord positions of the front and aft spars of the wingbox vary linearly with span in the wing and tail structures. The thickness of the tail structure is assumed to be constant. All structures are assumed to be made of an aluminium alloy with an allowable stress σ_{Allow} of 266 MPa. Table 2 shows the assumed quantities for the baseline definition.

Table 2: Assumed aerofoils and structural box limits for the baseline aircraft definition.

Item	Value
Root Aerofoil	SD7032
Tip Aerofoil	SD7037
Vtail Aerofoil	NACA0010
Box Limits @ root	15%-65%
Box Limits @ tip	25%-40%
Vtail Box Limits @ root	15%-50%
Vtail Box Limits @ tip	25%-40%
Vtail Box Thickness [mm]	1.5

The baseline configuration is then determined as the optimized result of an MDO procedure with design variables representing the wing spanwise twist distribution and the wingbox spanwise thickness distribution. Both distributions are assumed to be bilinear functions of the span position. The aircraft should maximize the load factor in cruise flight conditions while maintaining the structural mass below the 75Kg threshold without exceeding the allowable stress limit for the material and without degrading the aerodynamic efficiency (L/D) below 26. These mass and L/D limits are somewhat arbitrary and were chosen based on reasonability given the MTOW and AR of the aircraft (Corke, 2003). The optimization statement for this problem is:

$$\min_{x} f(x_1 \dots x_m) = -n\,(x_1 \dots x_m)$$

$$s.t. \qquad m_{wing}(x_1 \dots x_m) \leq 75$$

$$L/D(x_1 \dots x_m) \geq 26$$

With $\boldsymbol{x} = [x_1 \dots x_m]$ being the m design variables, n the maximum bearable load factor at MTOW, m_{wing} the wing mass in Kg and L/D the Lift over Drag value in cruise flight conditions and a half tank fuel load aircraft weight. For the baseline configuration, being a cantilevered wing with a continuous thickness distribution along the structure with a small number of variables describing it, the calculation of the maximum load factor is done by determining the AOA and lift at which the allowable stress in the wing structure is reached first and then build a surrogate model relating the load factor to the design variables directly. If a gradient based optimizer is used to solve the optimization problem this way, the gradients of the structural variables not affecting the maximum stress will be zero, therefore increasing the probability of discontinues gradients on the load factor function. Nevertheless, in this problem only one of the structural variables will be in this situation (root or tip thickness) and potential difficulties in getting an optimum result are tackled by starting the optimization with different initial design sets.

The two constraint functions are also surrogate based calculated. While the structural mass surrogate model is built directly from the sample results, the L/D surrogate model is based on the L/D values in cruise calculated for each configuration. This calculation for each configuration uses lift and drag obtained for specific AOA values (0,2,5 degrees) and linear and quadratic regressions are used to approximate the lift and drag vs AOA curves for a specific configuration and with these curves determine the cruise AOA and the corresponding L/D ratio in cruise. Therefore, the cruise condition of lift balancing weight in cruise is assumed to be approximated by the predictions of the surrogate model to a degree of accuracy that is to be assessed.

Table 3 lists the design variables, their boundaries and description.

Table 3: Design variables boundaries and description for the baseline MDO.

Design Variable	Boundaries	Description
DV1 [mm]	[2.0,5.0]	Thickness of box @ the wing root
DV2 [mm]	[1.0,3.0]	Thickness of box @ the break position
DV3 [mm]	[0.5,2.0]	Thickness of box @ the wing tip
DV4	[0.2,0.9]	Spanwise relative break position for the thickness distribution
DV5 [º]	[2.0,6.0]	Wing twist @ the wing root
DV6 [º]	[0.0,5.0]	Wing twist @ the break position
DV7 [º]	[-1.0,3.0]	Wing twist @ the wing tip
DV8	[0.25,0.8]	Spanwise relative break position for the twist distribution

3.2 SBW Configuration MDO

Similarly to the baseline configuration, the SBW configuration depicted in Figure 3 is assumed to have the same wingbox type of structure, fixed chord wise extension of the wingbox for the whole structure and fixed aerofoils shape. For the main wing part, the aerofoils are the same and vary in the same spanwise manner as the baseline wing. The tail, strut, horizontal tail and vertical tail aerofoils are constant NACA0010. The same structural material is used. Table 4 summarizes the assumptions for the design of this configuration.

Table 4: Assumed aerofoils and structural box limits for the SBW aircraft definition.

Item	Value
Root Aerofoil	SD7032
Tip Aerofoil	SD7037
Tail & Strut Aerofoil	NACA0010
Box Limits @ root	15%-65%
Box Limits @ tip	25%-40%
Strut Box Limits	25%-75%
Tail Box Limits	25%-75%

The configuration is now allowed to vary planform shape and area (although the main wing is still tapered) besides twist distribution, and several parameters define the structure thickness along its various segments. Figure 4 illustrates the structural design parameters used in the optimization of the configuration.

One can see from Figure 4 that the thickness distribution is not continuous along the structure. For the main wing, the inboard segment is defined by a constant thickness followed by a linear distribution for the outboard segment after the wing-strut joint. The strut thickness is constant from the joint to the beginning of the straight portion of the strut. Here there is discontinuity on the thickness distribution. Then the thickness varies linearly to and from the middle of that segment until the chord transition from the strut to the horizontal tail (HT) starts. Another linear thickness distribution is allowed in this transition until the HT tip. At this point a discontinuity in thickness is present and there is a linear distribution from HT tip to HT root and then from HT root/Vertical tail (VT) tip to VT root.

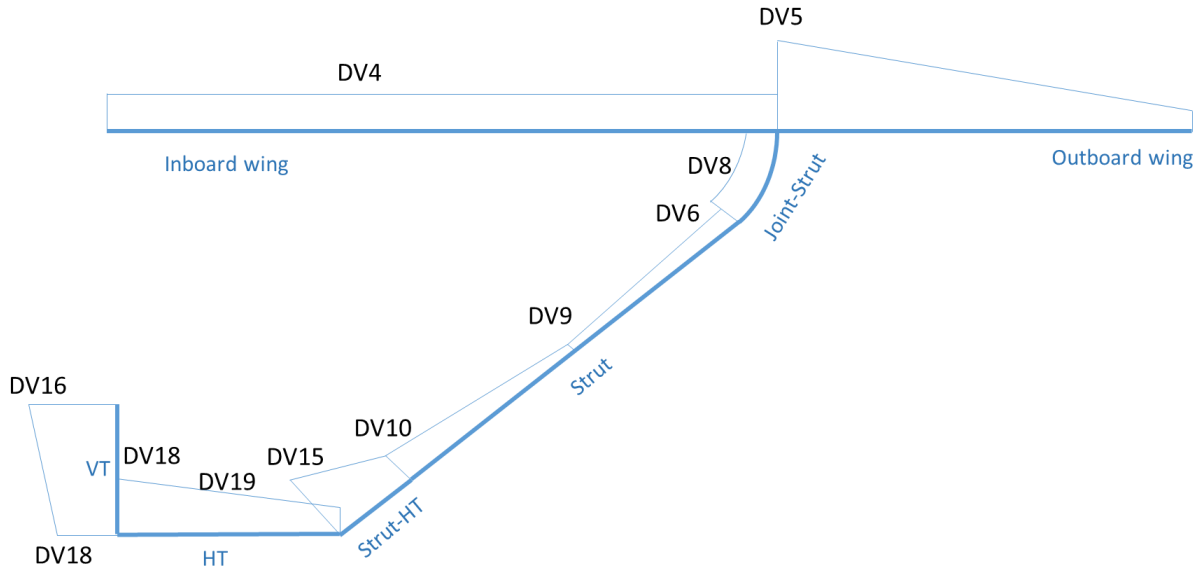

Figure 4: Front view schematic of the structural Design Variables (DV) for the SBW MDO.

Table 5 lists the design variables for the SBW optimization, their boundaries and description.

Table 5: Design variables boundaries and description for the SBW MDO.

Design Variable	Boundaries	Description
DV1	[0.9,1.1]	Area factor relative to the baseline
DV2	[0.9,1.5]	Aspect ratio factor relative to the baseline
DV3	[0.3,0.4]	Taper ratio
DV4 [mm]	[1.0,4.0]	Thickness of the inboard wing segment
DV5 [mm]	[1.0,3.0]	Thickness of the outboard wing segment @ the joint position
DV6 [mm]	[0.5,2.0]	Thickness of strut @ the beginning of wing-HT segment
DV7	[0.5,0.75]	Strut-Wing joint spanwise relative position
DV8 [mm]	[3.0,6.0]	Thickness of strut from joint to beginning of wing-HT segment
DV9 [mm]	[0.5,1.0]	Thickness of strut @ middle of wing-HT segment
DV10 [mm]	[0.5,2.0]	Thickness of strut @ end of wing-HT segment
DV11	[0.4,0.7]	Spanwise relative break position for the twist distribution
DV12 [°]	[3.0,5.0]	Wing twist @ the wing root
DV13 [°]	[1.0,4.0]	Wing twist @ the break position
DV14 [°]	[-1.0,2.0]	Wing twist @ the wing tip
DV15[mm]	[2.0,4.0]	Thickness @ end of strut-HT transition
DV16 [mm]	[2.0,7.0]	Thickness @ VT root
DV17	[0.4,0.6]	Strut chord relative to wing chord @ joint
DV18 [mm]	[1.0,4.0]	Thickness @ HT root/VT tip
DV19 [mm]	[0.5,1.0]	Thickness @ 2/3 HT spanwise position
DV20	[0.1,0.25]	Joint chordwise position relative to wing chord @ joint
DV21 [°]	[-5.0, 20.0]	Cruise AOA
DV22 [°]	[-5.0, 20.0]	Max n AOA

The MDO procedure for this configuration is similar to that of the baseline. The aircraft is intended to maximize the load factor subject to the same mass, stress and aerodynamic efficiency constraints as the baseline. The SBW optimization problem statement is as follows:

$$\min_{x} f(x_1 \dots x_m) = -n\,(x_1 \dots x_m)$$

$$s.t. \qquad m_{wing}(x_1 \dots x_m) \leq 75$$

$$L/D(x_1 \dots x_m) \geq 26$$

$$\sigma_{VM}^{i} \leq \sigma_{Allow} \qquad i = 1..l$$

$$\frac{\|L_{cr} - W_{cr}\|}{W_{cr}} \leq 0.5\%$$

With $\boldsymbol{x} = [x_1 \dots x_m]$ being the SBW m design variables, σ_{VM}^{i} represent the Von Mises stress at the ith control node, L_{cr} and W_{cr} are the lift and weight at the cruise point respectively. The other parameters have the same meaning as for the baseline configuration optimization.

Using the stress constraints prevents the zero gradient problem previously mentioned for the baseline configuration optimization which would be more severe in the SBW case, due to the more complex structure and the amount of structural design variables involved.

As can be noticed by the set of constraints for this problem, the load factor and the stress in the control nodes is now calculated based on the lift using the maximum load factor AOA as a variable to be determined during the optimization. Surrogate models of LF lift and σ_{VM}^{i} for specific AOA values (0,2,5 and 10 degrees) are generated and linear regressions are used to approximate the lift and σ_{VM}^{i} vs AOA curves and then obtain the load factor and stress constraints values.

Also, the cruise lift and the corresponding L/D ratio are calculated using the cruise AOA, which is a variable to be determined during the optimization. The L/D calculation uses now surrogate models of HF lift and drag for specific AOA values (0,2 and 5 degrees) and linear and quadratic regressions are used to approximate the lift and drag vs AOA curves for a specific configuration. With these curves one determines the cruise AOA and the corresponding L/D ratio in cruise. This approach is now forcing the cruise flight L=W condition explicitly and its accuracy is now dependent in the accuracy of the underlying lift and drag predictions.

4.0 RESULTS AND DISCUSSION

4.1 Quality of surrogate models

The baseline database for the HARW consist of 40 samples that are nearly evenly spread across the design space via an LHS. For each configuration an LF MDA analysis is performed for four different AOAs which in principle allow the interpolation of the results for the flight conditions of interest (cruise and maximum load). Of those 40 samples the most promising ones regarding weight and stress were selected to proceed with HF MDA analyses for the cruise flight condition. The enrichment of the data base with additional samples was done using only results of the surrogate based optimization process.

To reduce computational cost in the optimization process, sampling for the SBW configuration was done in a multistage approach. For each of the 80 sampled configuration the weight was determined. As the weight is a constraint in the optimization, samples with a weight higher than the boundary plus a margin (10%) were not evaluated with the LF MDA resulting in a total of 35 samples evaluated. This way only the regions of interest of the design space are explored. Within those samples 21 random sample results are computed using HF

MDA to assess the L/D in cruise conditions. Likewise to the HARW configurations, additional samples are added to the pool based on the results of the optimization.

For assessing the quality of LF based surrogate models, a cross validation method is used, where each sample of it is removed, a new reduced database is generated, and the removed sample is evaluated. The resulting maximum error for a single sample and the average error of the pool gives a measurement of the quality of the surrogate model. Table 6 shows the maximum and average error for the surrogate models for mass and maximum load factor for both configurations.

Table 6: Quality assessment of the surrogate models of the baseline.

Configuration	Surrogate model	Number of Samples	Maximum Error [%]	Average Error [%]
HARW	**Load Factor**	51	60.77	9.27
	Mass	51	10.00	2.33
SBW	**Load Factor**	89	58.70	16.31
	Mass	89	64.29	12.98

As one can see from the table, the average error for predictions based on the 51 samples for the baseline configuration is below 10%, and the mass prediction is below 2%. For the maximum error single higher values result in the prediction as the pool contains samples on the boundaries where the predictions are not accurate. Comparatively to the initial surrogate models based in 40 samples, the additional samples added to the pool during the optimization process did not show an improvement for the overall design space prediction. The reason for that is that they are located not widely spread across the design space but in an area of interest, resulting in an exploitation rather than an exploration.

Taking a closer look into the region of interest and restricting the error calculation to regions successively reduced around the calculated optimum, one can observe that the maximum and average error tend to reduce their magnitude. Therefore, as the optimization procedure progresses toward convergence, the surrogate quality in what is expected to be the region of interest increases.

Another potential improvement in surrogate quality with an increasing data base of samples is the possibility of increasing the order of the regression model used in the Kriging model building. Through another cross validation using the extended pool it was found a higher order regression did not provide benefits in the prediction, neither for the average nor the maximum error improvement.

4.2 Samples results

4.2.1 HARW Configuration

Figure 5 and 6 below show the samples results for the maximum load factor and cruise L/D versus the wing structure mass. One can observe a trend of load factor increase with structure mass in Figure 5, as expected. It also shows a degree of dispersion of the data, which is also to be expected, since the maximum load is dependent on the stress of one part of the structure which is the first to exceed the stress while everywhere else the structural thicknesses can change within some margin, leading to different structural masses.

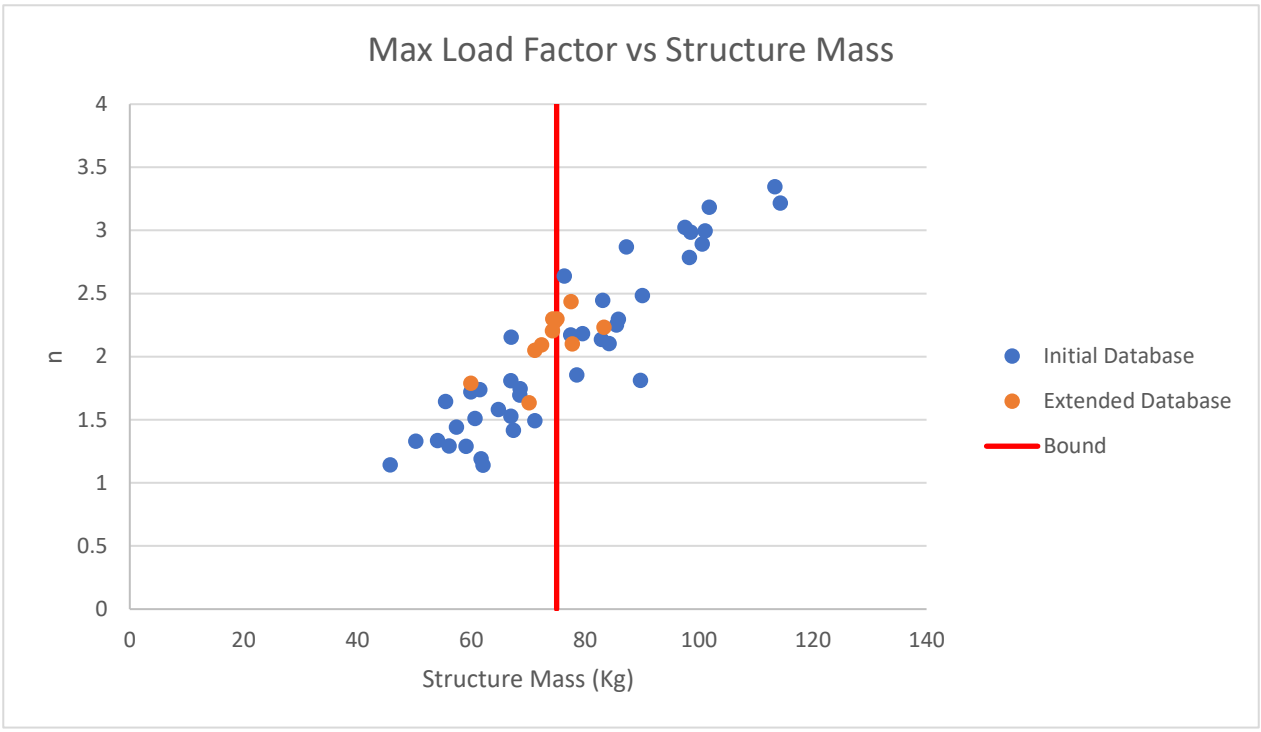

Figure 5: Maximum Load Factor vs Wing Structure Mass for the HARW configuration samples.

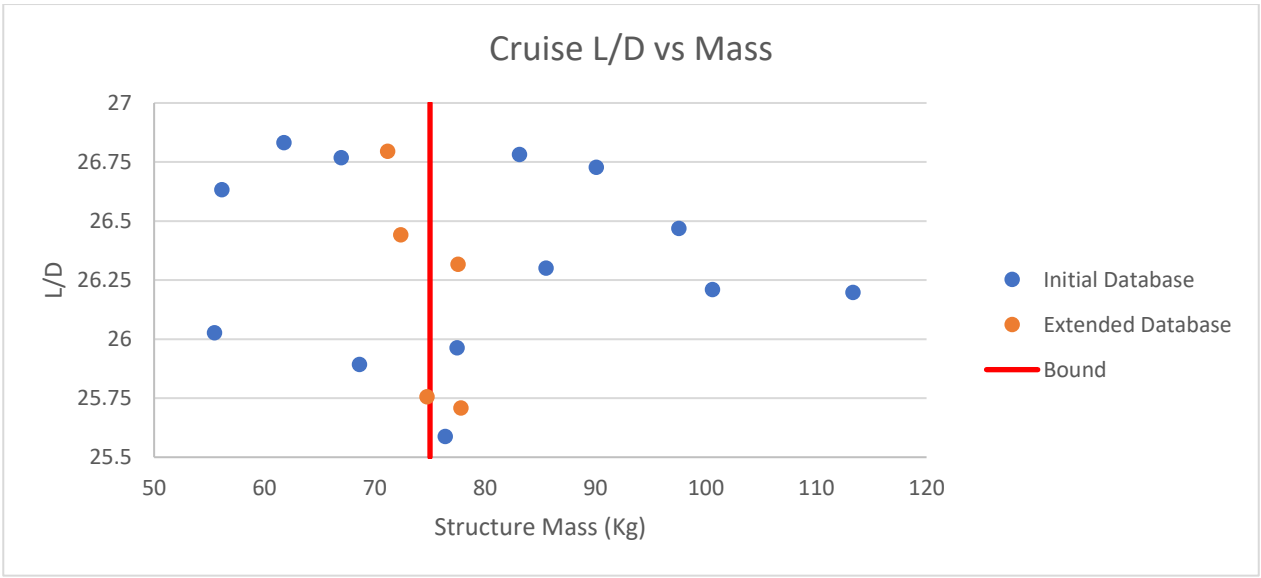

Figure 6: Cruise L/D vs Wing Structure Mass.

Figure 6 shows the HF results for the samples used for this kind of analysis. No particular trend is identified in this figure. Given that the wing planform is unchanged, the dispersion of the data suggests that deformation and twist distribution play a role in the cruise L/D, as they should, although the L/D variation within the sample is around 5%.

4.2.2 SBW Configuration

Figure 7 and 8 show the maximum load factor versus structure mass and the cruise L/D versus AR respectively.

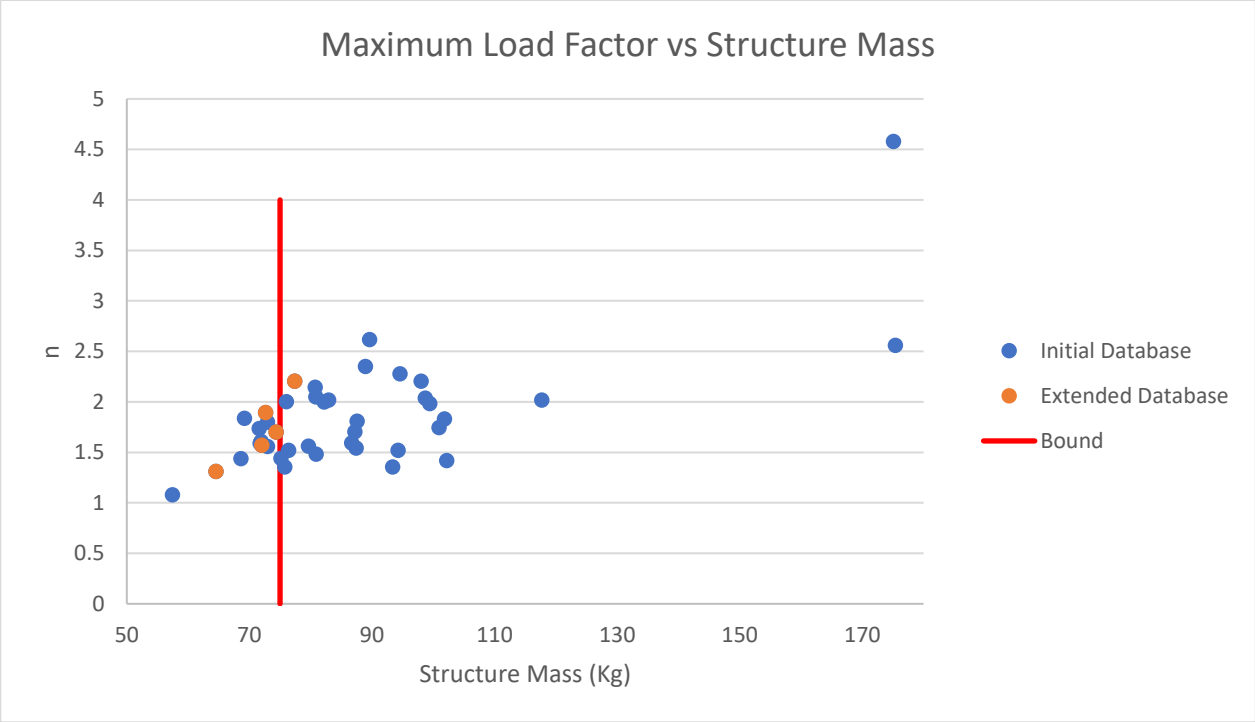

Figure 7: Maximum Load Factor vs Wing Structure Mass for the SBW configuration samples.

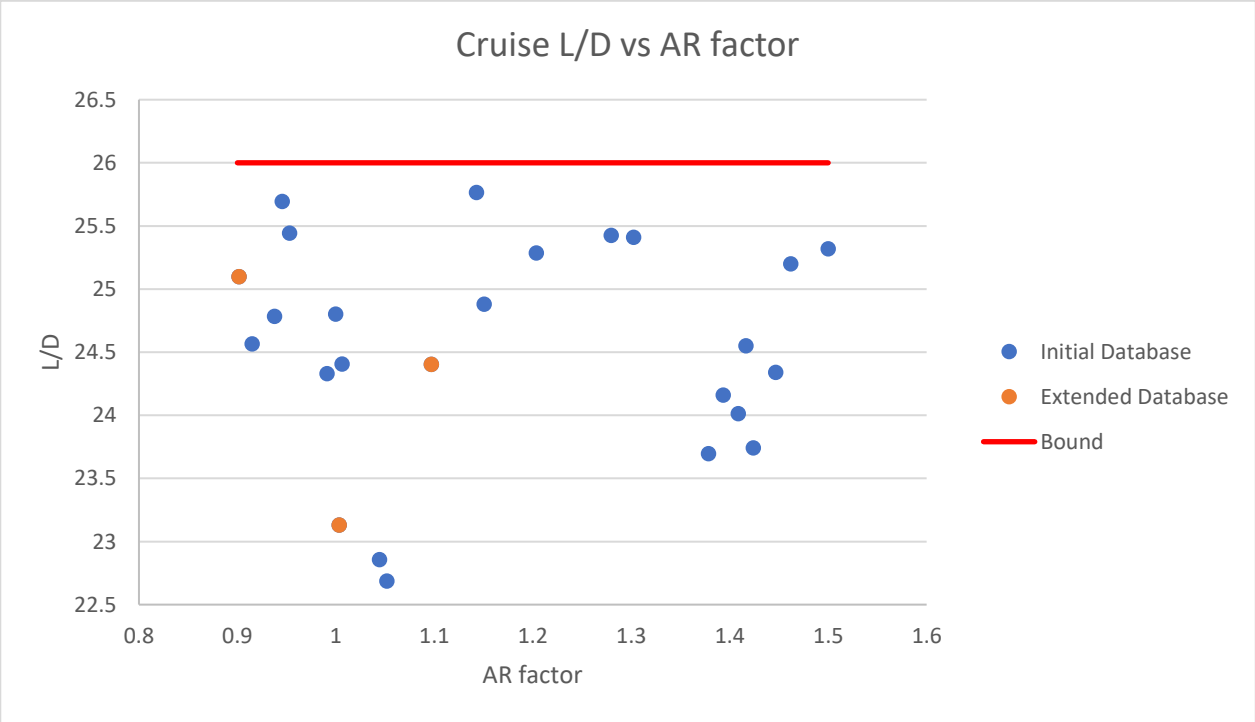

Figure 8: Cruise L/D vs Wing Structure Mass for the SBW configuration samples.

One cannot observe a trend between maximum load factor and structure mass for the SBW as was observable for the HARW. One possible explanation is that the complexity of the structure and the increased number of structural variables increase the dispersion of the results relatively to the HARW configuration.

Note the two highest mass samples present in the pool. These where analysed to understand the maximum load that this structure would be able to bear if no mass restrictions would exist. One has the same AR as the HARW while the other has an AR 1.5 times higher. As a result, the load bearing capability of the later is significantly reduced in comparison.

The results in Figure 8 are counter intuitive in the sense that one is expecting the induced drag to be reduced as AR increases and no trend can be identified from the results. Furthermore, the defined requirement for an L/D of 26 is not fulfilled by any of the HF analysed samples. In order to understand the reasons this rigid aircraft HF simulations were performed on samples with varying AR. Table 7 shows the L/D results of samples #9 and #12 with AR factors of 1.4 and 0.94 respectively, for rigid and deformed shapes simulations and AOAs of 0,2 and 5 degrees:

Table 7: Comparison of rigid vs deformed L/D results for the two different AR samples.

SBW sample #	Rigid	Deformed	Error [%]
#9 AR factor=1.4	24.32	22.46	7.6
	26.25	24.04	8.4
	20.06	19.43	3.1
#12 AR factor=0.94	23.63	24.12	-2.1
	24.47	24.32	0.6
	18.93	18.52	2.1

The results in Table 7 show that for the rigid analysis the sample with higher AR has a higher L/D, therefore as expected in theory. Nevertheless, it also shows that the effect of deformation in the higher AR is of higher magnitude than for a lower AR. Therefore, it seems that although the extra drag due to the presence of the strut in the SBW configuration is balanced by the AR increase as hypothesised, the deformation of the structure seems to degrade the aerodynamic performance significantly.

4.3 Comparison of final configurations

4.2.1 HARW Configuration

At the current status of the optimization, the best feasible sample (#46) obtained so far that respects the constraints is calculated to bear a load factor of 2.09, having a mass of 72.365Kg and with a cruise L/D of 26.44.

The stress distribution at the maximum load condition for this sample is shown in Figure 9 as well as the twist and thickness distributions along span.

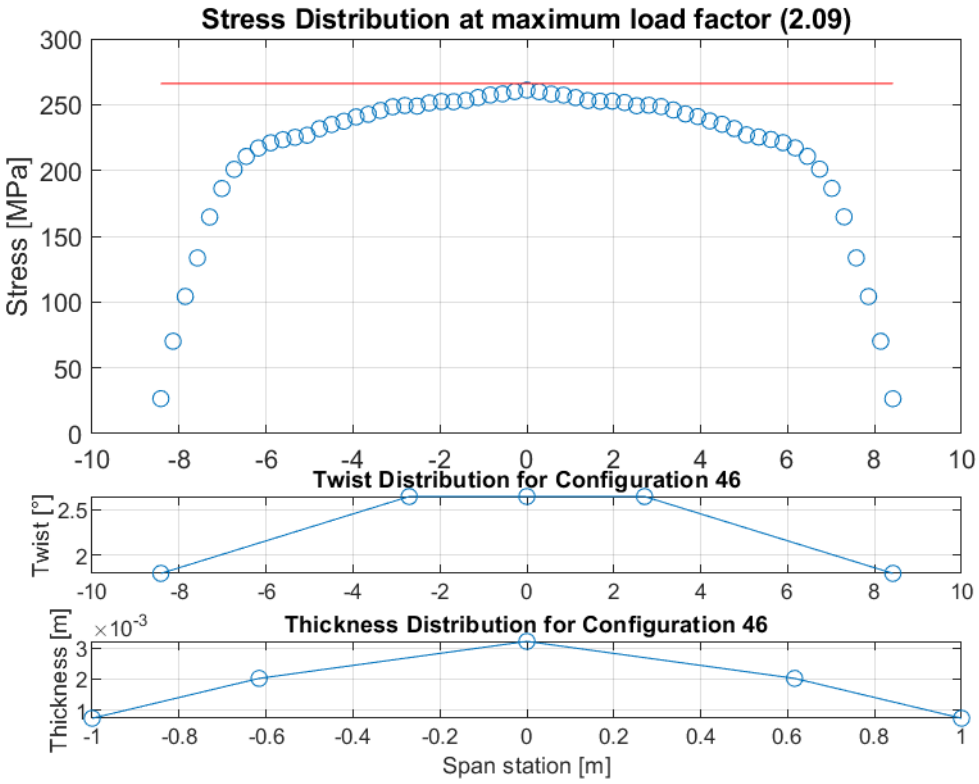

Figure 9: Stress, twist and thickness distributions of the HARW current best feasible sample.

It would be expected that a somewhat higher load factor can be achieved with a higher structural mass even at the expense of a degradation in L/D. In fact, the last sample analysed (#51) exceeds the maximum mass constraint with a mass of 77.548Kg but also improves the load factor. Figure 10 shows the configuration results.

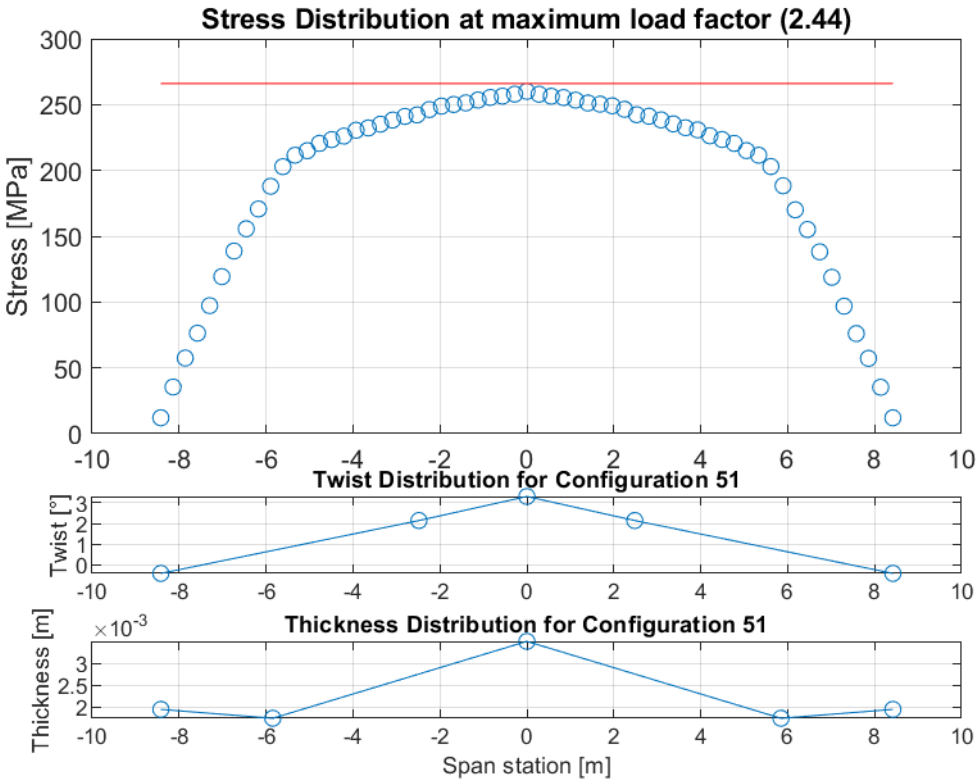

Figure 10: Stress, twist and thickness distributions of the HARW last analysed sample.

The prediction vs analysis results for sample #51 are shown in Table 8.

Table 8: Comparison of prediction and analysis results for the last analysed sample.

HARW sample #	Parameter	Surrogate model	Analysis	Error [%]
51	**Load Factor**	2.28	2.44	6.33
	Mass	77.46	77.55	0.12
	L/D	26.15	26.32	0.64

4.2.2 SBW Configuration

As stated before the SBW configuration proposed did not comply with the L/D requirement for any of the analysed samples so far. Thus, the configuration selection of the best available sample is somewhat arbitrary. The choice was made on sample #81 which has a similar mass to the HARW (72.688Kg), a cruise L/D of 24.40 and a maximum load factor of 1.89. Comparing to the HARW planform, this sample increases the AR by 10% and reduces wing area by 4%.

Figure 11 shows the deformed shape and pressure distribution LF FSI results and the nodal displacement of the structural model for the maximum load factor of the SBW #81 sample. Figure 12 shows a plot of the stress distribution for that same load case.

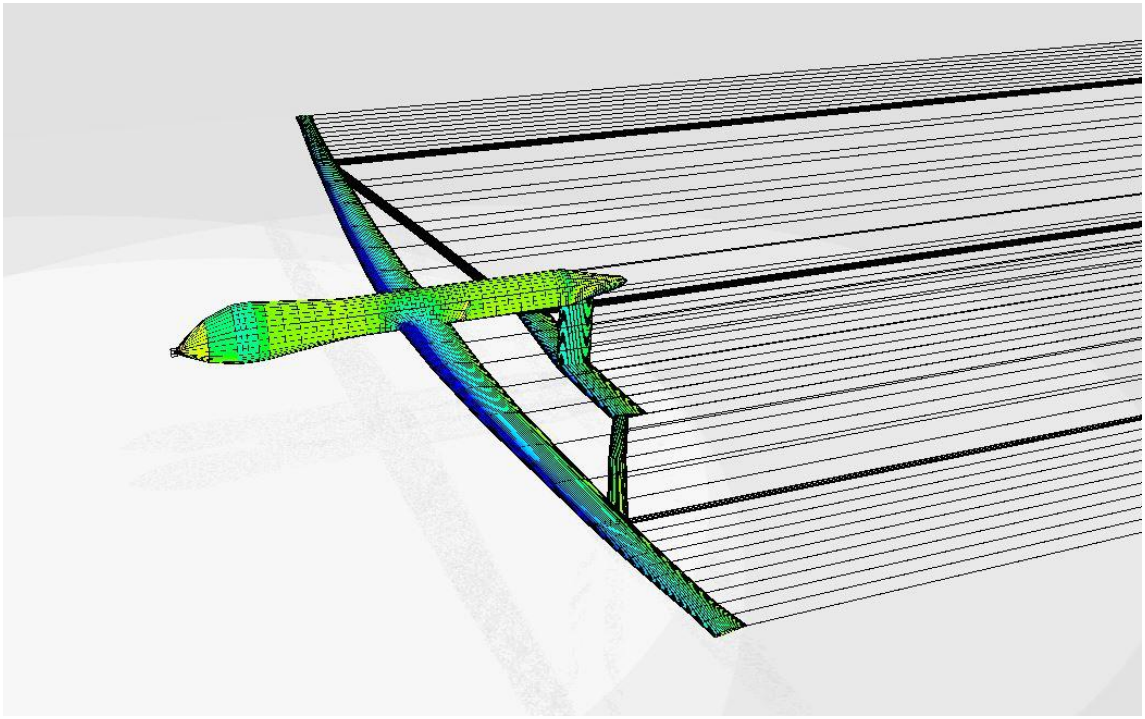

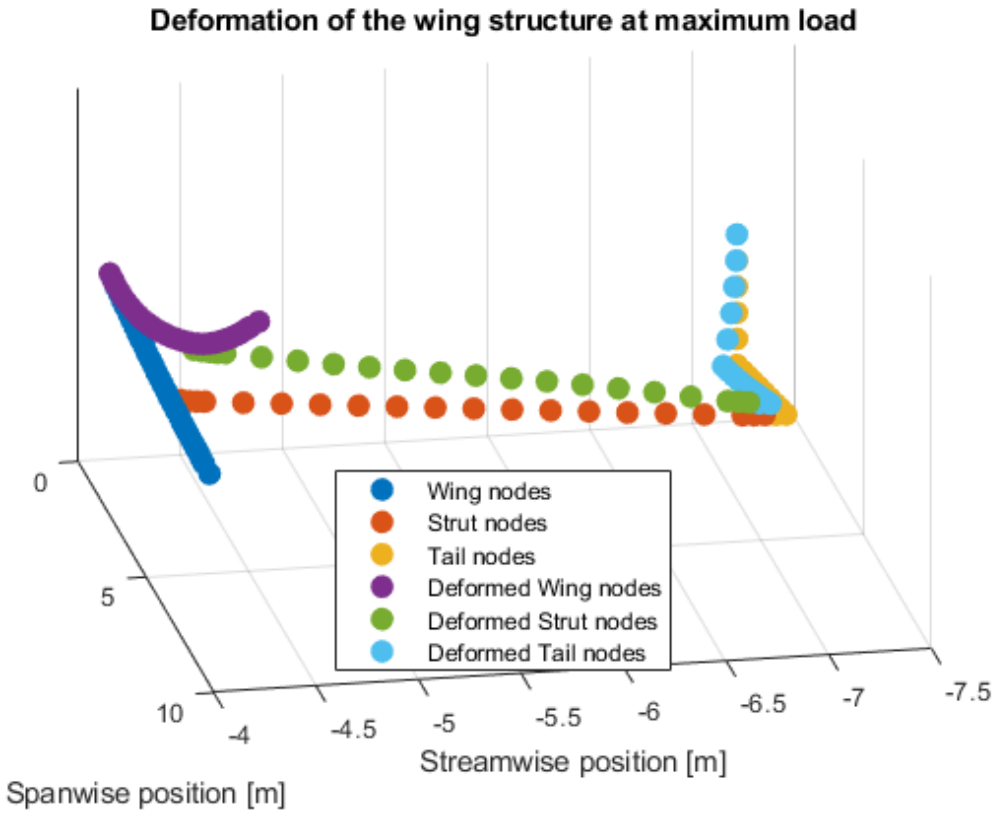

Figure 11: Deformed shape and pressure distribution LF FSI results (up) and structural model deformed shape vs undeformed shape (down) for the SBW #81 sample.

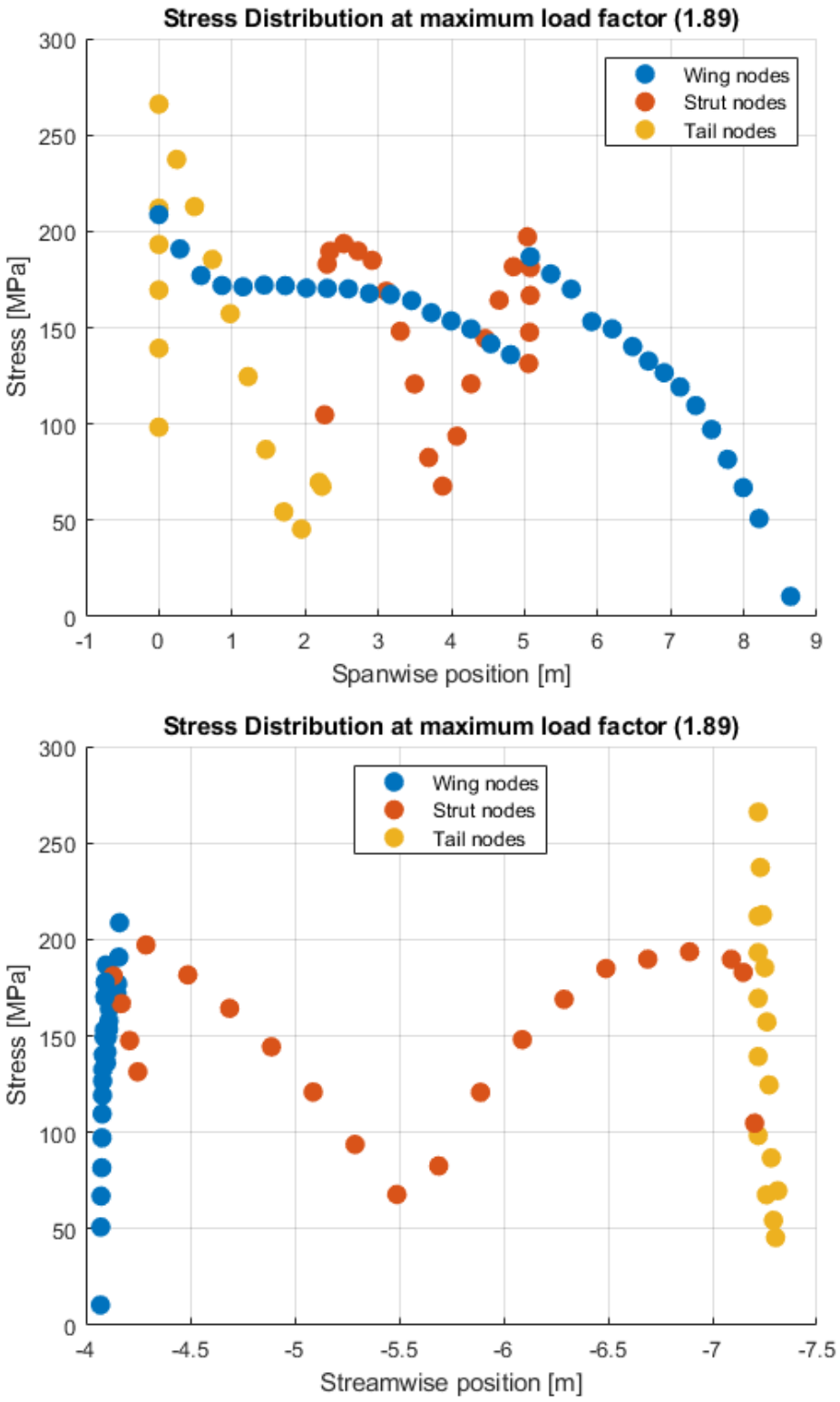

Figure 12: Stress distribution in the spanwise (up) and streamwise (down) directions for the SBW #81 sample at maximum load case.

One can notice from Figure 12 that the stress limit is reached in the tip of the VT/root of the HT. Nevertheless, the maximum thickness limit at that point of the structure is still far from reached as can be seen in Table 9 below. The structure could therefore be reinforced in this region and increase the load factor. The question remains if the resultant deformation would help improve the L/D value.

Figure 11 above shows the deformed versus undeformed nodal positions of the structural model for the maximum load factor. One can observe that the wing is pushed aft by the strut while bending upwards. In the cruise flight case, this is likely to cause a twist down and reduce the load on the outboard part of the wing, leading to a change on the lift distribution that jeopardises the gains from the AR increase. A better tuning of the undeformed twist distribution and chordwise strut position might help mitigate this problem at the expense of higher number of samples and related computational time. Table 10 below shows that the surrogate errors are still high with the generated database and that it could use further samples.

Table 9 shows the numerical values for the design variables of the SBW sample #81:

Table 9: SBW #81 sample design variables.

Sample #	DV1	DV2	DV3	DV4	DV5	DV6	DV7
81	0.960	1.097	0.374	1.713mm	1.442mm	1.262mm	0.588
DV8	**DV9**	**DV10**	**DV11**	**DV12**	**DV13**	**DV14**	**DV15**
3.876mm	0.674mm	1.282mm	0.556	4.109º	1.974º	-0.027º	2.979mm
DV16	**DV17**	**DV18**	**DV19**	**DV20**	**DV21**	**DV22**	
3.424mm	0.476	1.578mm	0.719mm	0.173	1.75º	8.00º	

Table 10: Comparison of prediction and analysis results for the SBW #81 sample.

SBW sample #	Parameter	Surrogate model	Analysis	Error [%]
81	**Load Factor**	1.69	1.89	-10.58
	Mass	70.893	72.688	-2.47
	L/D	22.07	24.40	-9.50

Unfortunately, the reduced number of database extension samples obtained so far do not allow definite conclusions on if the increase in AR denies this configuration to actually increase the load bearing capability without mass increase or penalties in aerodynamic efficiency but these results show that it should be hard to comply with the L/D requirement and that a potential benefit in the maximum load factor for this configuration does not appear to become significant. Table 11 below supports these affirmations by compiling the selected results for the two configurations.

Table 11: Comparison of SBW and HARW selected samples.

Configuration	Sample #	Area Factor	AR factor	Mass (Kg)	L/D	n
HARW	46	1.0	1.0	72.365	26.44	2.09
HARW	51	1.0	1.0	77.548	26.32	2.44
SBW	81	0.96	1.10	72.688	24.40	1.89

5.0 CONCLUSIONS

An SBW configuration was proposed in order to improve the manoeuvrability of surveillance/combat drone. A surrogate model-based optimization framework was used in the MDO of a HARW and an SBW configurations based on the Predator drone and allow a comparison between the two. Both configurations were optimized for maximum load factor bearing capability while maintaining minimal aerodynamic efficiency and maximal structural mass.

The surrogate model-based optimization resorted to LF and HF FSI calculations for each configuration. In order to reduce the number of HF evaluations, engineering judgement was used to decide which samples should be used to build the HF based aerodynamic surrogate models and avoid exploring regions that do not appear of interest.

The HARW configuration was optimized to some extent, although it would benefit from increased number of samples to improve the converge the optimized result. This problem is simpler than the SBW optimization problem in dimensionality and structural complexity.

Sample results show that deformation has an impact on aerodynamic efficiency for the SBW configuration, since no trend could be identified with varying AR. Furthermore, the increase in AR seems to possibly compensate the increased drag from the strut presence in a rigid configuration, but the associated deformation appears to introduce significant drag increase.

As the initial sample did not provide high enough L/D values, an optimized result could not be obtained for the SBW at this point. An arbitrary sample was selected as the “best” sample available for comparison with the HARW configuration.

The comparison shows that, at the light of current results, it is unlikely that the proposed configuration will render significant benefits in load bearing capability even with reasonable degradation of aerodynamic efficiency or structural mass. Further results will allow for a final assessment on this subject.

6.0 REFERENCES

Abbas, A., de Vicente, J., Valero, E., 2013. Aerodynamic technologies to improve aircraft performance. Aerospace Science and Technology 28, 100–132. https://doi.org/10.1016/j.ast.2012.10.008

Biles, W.E., Kleijnen, J.P.C., Beers, W.C.M. van, Nieuwenhuyse, I. van, 2007. Kriging metamodeling in constrained simulation optimization: an explorative study, in: 2007 Winter Simulation Conference. Presented at the 2007 Winter Simulation Conference, pp. 355–362. https://doi.org/10.1109/WSC.2007.4419623

Carrier, G., Atinault, O., Dequand, S., Toussaint, C., 2012. Investigation of a Strut-Braced Wing Configuration for Future Commercial Transport, in: 28th Congress of the International Council of the Aeronautical Sciences. Presented at the ICAS, Bonn.

Cavallaro, R., Demasi, L., 2016. Challenges, Ideas, and Innovations of Joined-Wing Configurations: A Concept from the Past, an Opportunity for the Future. Progress in Aerospace Sciences 87, 1–93.
Corke, 2003. Design of Aircraft.
Dowell, E., Edwards, J., Strganac, T., 2003. Nonlinear Aeroelasticity. Journal of Aircraft 40, 857–874. https://doi.org/10.2514/2.6876
Forrester, A.I.J., Sbester, A., Keane, A.J., 2008. Engineering Design via Surrogate Modelling. John Wiley & Sons, Ltd, Chichester, UK. https://doi.org/10.1002/9780470770801
Katz and, J., Plotkin, A., 2004. Low-Speed Aerodynamics, Second Edition. Journal of Fluids Engineering 126, 293–294. https://doi.org/10.1115/1.1669432
Kleijnen, J.P.C., van Beers, W., van Nieuwenhuyse, I., 2012. Expected improvement in efficient global optimization through bootstrapped kriging. J Glob Optim 54, 59–73. https://doi.org/10.1007/s10898-011-9741-y
Oden, J.T. (Ed.), 1975. Computational mechanics: International Conference on Computational Methods in Nonlinear Mechanics, Austin, Texas, 1974, Lecture notes in mathematics. Springer, Berlin.
Sigrist, J.-F., 2015. Fluid-structure interaction: an introduction to finite element coupling. Wiley, Chichester, West Sussex, United Kingdom.
Wang, G.G., Shan, S., 2007. Review of Metamodeling Techniques in Support of Engineering Design Optimization. Journal of Mechanical Design 129, 370–380. https://doi.org/10.1115/1.2429697
Wolkovitch, J., 1986. The joined wing - An overview. Journal of Aircraft 23, 161–178. https://doi.org/10.2514/3.45285
Zhang, Y., Kim, N.H., Park, C., Haftka, R.T., 2018. Multifidelity Surrogate Based on Single Linear Regression. AIAA Journal 56, 4944–4952. https://doi.org/10.2514/1.J057299

[1] https://en.wikipedia.org/wiki/General_Atomics_MQ-1_Predator

7.0 ACKNOWLEDGEMENTS

We acknowledge the support of the Natural Sciences and Engineering Research Council of Canada (NSERC)